# Indoor Navigation Using Asynchronous Pseudolites

Daniele Borio, Ciro Gioia
Institute for the Protection and Security of the Citizen, IPSC
EC Joint Research Centre
Ispra, Italy
{daniele.borio, ciro.gioia}@jrc.ec.europa.eu

***Abstract*—Indoor navigation using Global Navigation Satellite System (GNSS) signals is a challenging task which involves the solution of several problems such as signal attenuation, fading and measurements biases due to multipath propagation. A possible solution is represented by pseudolites or pseudo-satellites which have been considered for their ability to provide GNSS-like signals. In this paper, the potentialities of asynchronous pseudolites are investigated with the final goal of reducing the number of transmitters and increasing the accuracy of the system with respect to proximity-based techniques. An asynchronous pseudolite system has been implemented using Universal Software Radio Platforms (USRPs) and tested in a deep indoor environment. Carrier-to-Noise power spectral density ratio ($C/N_0$) measurements were obtained from the pseudolite signals and processed using a Least Squares (LS) approach. An improved algorithm was also design to take into account the quality of the different measurements. From the experiments, it emerged that $3$ pseudolites are sufficient to enable indoor navigation in an office area of about $350$ square meters with meter level accuracy. These results are particularly encouraging since they were obtained without exploiting map constraints and prior knowledge of the user position.**

***Keywords*—asynchronous signals, GNSS, indoor navigation, pseudolite, Received Signal Strength, RSS**

## I. Introduction

Indoor navigation using Global Navigation Satellite System (GNSS) signals is a challenging task which involves the solution of several problems such as signal attenuation, fading and measurements biases due to multipath propagation. Although High-Sensitivity (HS) GNSS receivers significantly extended the range of operation of satellite-based positioning, effective navigation in difficult scenarios such as buildings made of concrete is still precluded. Despite the significant progress brought by HS techniques, indoor navigation based only on GNSS signals seems to be unfeasible and a possible way to fill this gap is the integration with other technologies. To provide seamless outdoor/indoor navigation, several solutions have been proposed such as the integration of inertial sensors, the exploitation of signals of opportunity and the deployment of additional infrastructures dedicated to GNSS augmentation. Among the technologies developed for indoor GNSS augmentation, pseudolites or pseudo-satellites [1] have been considered for their ability to provide GNSS-like signals which could be used with minimal receiver hardware changes [2]. Several pseudolite systems have been developed mainly exploiting the same operational principles of GNSS: pseudolites are synchronized to a single time scale and pseudolite signals are used to compute travel times and pseudoranges which are finally used to compute the user position [3]. In this case, hybrid pseudolite/GNSS positioning can be achieved by estimating the time difference between GNSS and pseudolite time scales or by synchronizing the pseudolites to the GNSS time scale.

The development of such type of pseudolite system is however characterized by stringent synchronization requirements which may lead to significant deployment costs. Moreover, biases in the measurements could still be present due to multipath propagation. For these reasons, a second class of pseudolites operating in an asynchronous way has been recently suggested. In particular, the Japanese Aerospace Exploration Agency (JAXA) proposed the exploitation of the proximity principle where pseudolites are used as sources of reference positions [4], [5]. In this case, a dense network of devices is deployed and each device operates independently, continuously broadcasting its position. The signal transmitted by each device has very low power and can only be received in a limited region of space. In this region, the receiver should be able to acquire and process a very limited number of signals (ideally one). The receiver position is then determined as the position of the transmitter broadcasting the strongest received signal. This concept has been used for the development of the Indoor MEssaging System (IMES) that will be the indoor extension of the Quasi-Zenith Satellite System (QZSS). It is noted that the proximity principle provides a limited accuracy corresponding to the area covered by a single IMES transmitter [4], [5]. In particular, IMES is suitable for applications where room identification is sufficient and an accuracy of about 5 meters is required.

The proximity principle does not allow the full exploitation of the potentialities of an asynchronous pseudolite system. For this reason, the main objectives of this paper are the analysis and demonstration of indoor navigation using a network of asynchronous pseudolites. In particular, techniques based on Received Signal Strength (RSS) have been considered and implemented. The final goal is to reduce the number of transmitters, for the same coverage area, and increase the accuracy of the system with respect to proximity-based techniques.

For the analysis, asynchronous pseudolites have been implemented on Universal Software Radio Platforms (USRPs) and deployed in a building on the campus of the Joint Research Centre (JRC) in Ispra (VA, Italy). The USRP pseudolites broadcast signals similar to the GPS L1 Coarse/Acquisition (C/A) modulation where a pulsing scheme has been introduced to reduce interference and near-far problems [6], [7].

For the signal reception, a measurement unit comprising a HS sensitivity u-blox LEA-6T receiver and a Realtek RTL2832U front-end was assembled. In this way, it was possible to obtain Carrier-to-Noise power spectral density ratio ($C/N_0$) observations from two independent sources. The u-blox receiver was used to obtain $C/N_0$ measurements which are directly proportional to the RSS of the pseudolite signals [8]. The u-blox receiver was able to process the signals from the USRP pseudolites and provide valid C/N0 measurements.

The Realtek RTL2832U device is a low-cost TV tuner which can be used, with some software modifications, to collect raw In-phase/Quadrature (I/Q) samples. In this case, a dedicated software interface was developed to collect raw GPS and pseudolite signals. From the I/Q samples it was then possible to extract RSS measurements. In this way, two independent sources of measurements were available. Moreover, the availability of raw I/Q samples allowed the characterization of the signals transmitted by the USRP devices and the implementation of dedicated Software Defined Radio (SDR) techniques for the processing of pulsed pseudolite signals [6]. $C/N_0$ measurements were then processed using a Least Squares (LS) approach where RSS measurements expressed on a logarithmic scale are related to the user and pseudolite positions. The propagation parameters required for relating the user position to the RSS observations were obtained during a calibration phase, as described in Section IV-A, and can be transmitted as part of the pseudolite navigation message. This type of approach is generally used for indoor positioning, for example using WiFi signals [9], [10], and it is adapted here to pseudolites. This standard approach has been then modified to take into account the different quality of the RSS measurements. More specifically, $C/N_0$ also provides an indication of the quality of the measurements and thus a weighted LS approach was developed to further improve the performance of RSS positioning. This approach can be considered an extension of the algorithm discussed in [9], [10] which requires an estimate of the measurement variance.

Several measurement campaigns were conducted, and the accuracy of the system was assessed using reference points where the user was required to stay stationary for a few seconds. The position obtained using pseudolite RSS measurements was then compared against reference values. From the experiments, it emerged that three pseudolites are sufficient to enable indoor navigation in an office area of about 350 square meters. The accuracy of the position fixes depends strongly on the geometry defined by the locations of the pseudolites. In particular, the building concerned has an elongated shape and offices are placed symmetrically along a central corridor of about 36 metres. The pseudolites were placed in three different offices and a poor geometry was obtained along the direction perpendicular to the central corridor. For this reason, an accuracy of about 5 meters was obtained along this direction. The accuracy along the corridor direction was five times better: position errors lower than 1 metre were obtained. These results are particularly encouraging, since they were obtained without exploiting map constraints and prior knowledge of the user position.

The remainder of this paper is organized as follows: the architecture of the asynchronous pseudolite system developed is briefly summarized in Section II whereas the receiving equipment assembled for the data collections is described in Section III. Section IV details the standard and weighted LS algorithms adopted for evaluating the user position and sample experimental results are provided in Section V. Finally, Section VI concludes the paper.

## II. Asynchronous Pseudolite System

The potentiality of asynchronous pseudolite systems were tested by deploying a system of three pseudolites on the first floor of a building of the JRC campus. The pseudolites were implemented on USRP II platforms and additional details on their architecture can be found in [6]. In [6], a single pseudolite was considered and tests were conducted in an

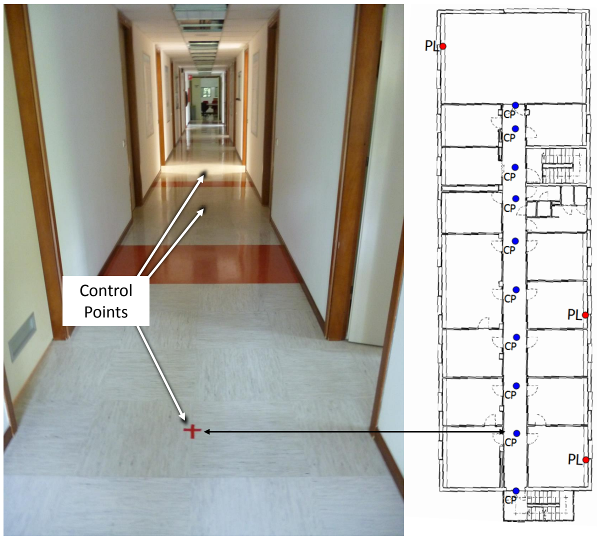


Fig. 1. Location of the pseudolites and control points on the first floor JRC building used for the testing.

TABLE I
PARAMETERS ADOPTED FOR THE TRANSMISSION OF THE PSEUDOLITE SIGNALS.

| Parameter | Value |
|---|---|
| Modulation Type | Pulsed |
| Codes | Gold Code / GPS L1 C/A |
| Duty Cycle | 10 % |
| Pulsing Scheme | Uniform [7] |
| Sampling/generation frequency | $f_s = 2.5$ MHz |

anechoic chamber. In this paper, three pseudolites were deployed in a realistic environments such as the first floor of an office building. The floor was thoroughly surveyed and geo-referenced control points were placed along the main corridor. The USRP pseudolites were deployed in three different offices as shown in Fig. 1. Pseudolites are indicated in a progressive order starting from the bottom of the floor plan in Fig. 1. Thus pseudolite 1 is placed in the bottom right office, closest to the fire escape stairs, whereas pseudolite 3 is in the large conference room at the end of the corridor. Pseudolite 2 was placed in the middle of the floor. This pseudolite placement guarantees a good geometrical distribution of the transmit devices along the North-South direction. On the contrary poor geometrical conditions are obtained along the East-West direction. This fact will be reflected in the results presented in Section V.

The signals transmitted by the three asynchronous pseudolites were generated according to the algorithm developed in [7], with the parameters listed in Table I. In particular, pulsed signals were generated using a 10 % duty cycle as for the

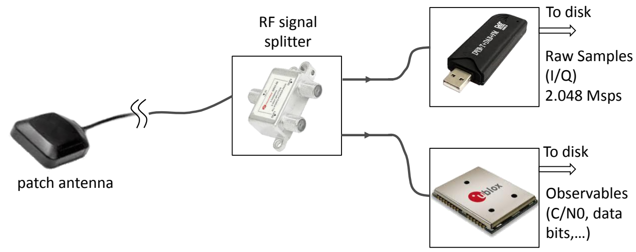


Fig. 2. Measurement unit assembled for the data collection. A Realtek RTL2832U front-end and a u-blox LEA-6T receiver were connected to the same GPS antenna and used to collect raw I/Q samples and pseudolite signal measurements.

TABLE II
SETTINGS ADOPTED FOR THE REALTEK RTL2832U DEVICE USED AS A GNSS DATA GRABBER.

| Parameter | Value |
|---|---|
| Sampling frequency | $f_s = 2.048$ MHz |
| Centre frequency | 1575.42 MHz |
| Sampling Type | Complex I/Q |
| No. of bits | 8 |

standard considered in [11]. The base signals, generated before the addition of the pulsing sequence, have the same format as that adopted for the GPS L1 C/A signal. This made it possible to use a commercial HS receiver for the processing of pseudolite signals.

## III. RECEIVING EQUIPMENT

The measurement unit adopted for the reception of pseudolite signals was made of a Realtek RTL2832U front-end and a u-blox LEA-6T receiver connected to the same GPS patch antenna. A schematic representation of the measurement unit used for data collections is shown in Fig. 2.

The Realtek RTL2832U device was configured to operate according to the settings reported in Table II and adapted to collect raw I/Q GPS and pseudolite signals. A custom software, the JRC Interference Monitor (JIM), was developed and interfaced to the Realtek RTL2832U device to collect I/Q samples and monitor the histogram and Power Spectral Density (PSD) of the data. Examples of operations of the JIM software are shown in Fig. 3. In Fig. 3 a) the histogram and PSD are computed in the absence of pseudolite signals: the histogram has a bell shape and reveals the presence of noise only, whereas the PSD is almost flat with a central peak due to imperfections in the Realtek front-end (residual DC offset and I/Q imbalances). In Fig. 3 b), the JIM software is operating in the presence of pseudolite signals. The histogram is now characterized by low side peaks corresponding to

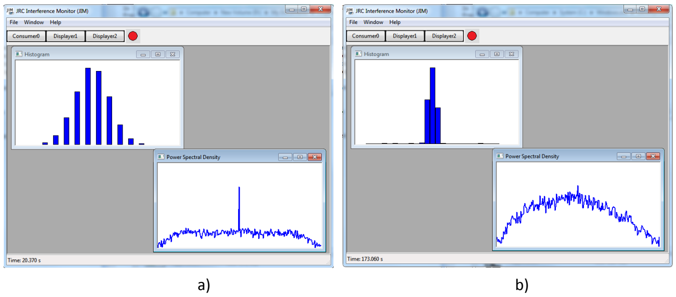


Fig. 3. Histogram and PSD of the samples streamed using the Realtek RTL2832U device. a) Pseudolite signal absent. b) Pseudolite signal present.

the pseudolite pulses. The PSD is characterized by a bell shape, corresponding to the main lobe of the spectrum of the pseudolite signal. The u-blox LEA-6T receiver was adopted for its ability to acquire and track the signals generated by the USRP pseudolites. In this work, only $C/N_0$ measurements were used. The Realtek RTL2832U device and u-blox LEA-6T receiver were packaged in a single box and placed in a backpack which was carried by the user along with a laptop. The Realtek RTL2832U device and the u-blox LEA-6T receiver were directly powered through the USB ports of the laptop and no additional power supply was required.

## IV. Standard and Weighted RSS Positioning

According to [12], RSS is defined as the voltage measured by a receiver's RSS Indicator (RSSI) circuit and corresponds to the measured power on a logarithmic scale. RSS measurements are usually modeled as [13]:

$$P(d) = P_0 - 10\alpha \log_{10} \frac{d}{d_0} \tag{1}$$

where $P(d)$ is the RSS measured at the distance $d$ from the emitter. $\alpha$ is the path-loss exponent and $P_0$ is the power received at a short reference distance, $d_0$. Note that RSS measurements are expressed in logarithmic units.

RSS based techniques are widely used because RSS is easy to measure. In particular, RSS values can be obtained from, for example

- the Automatic Gain Control (AGC) levels [14], [15];
- $C/N_0$ measurements [8].

In this paper, $C/N_0$ measurements are used as basis for RSS positioning. In particular, (1) can be rewritten in terms of $C/N_0$:

$$\left(\frac{C}{N_0}\right)_i = K_i - \alpha 10 \log_{10}(d_i) \tag{2}$$

where the index, $i$, has been added to denote $C/N_0$ measurements from the $i$th transmitter and $K_i$ is a constant accounting for the power of the $i$th transmitted signal and the reference distance $d_0$. Unless specified, $C/N_0$ will always be expressed in units of dB-Hz.

When the constants $K_i$ and $\alpha$ are known, it is then possible to establish a direct relationship between the measured $C/N_0$ and transmitter-receiver distance. In turn, this distance can be expressed as a function of the user position:

$$d_i = \sqrt{(x_u - x_i)^2 + (y_u - y_i)^2} \tag{3}$$

where $(x_u, y_u)$ and $(x_i, y_i)$ are the coordinates of the user and the $i$th pseudolite , respectively. Although (3) considers the case of 2D positioning, the 3D case can be easily obtained. Using (3), it is possible to rewrite (2) as

$$\left(\frac{C}{N_0}\right)_i = K_i - \frac{1}{2}\alpha 10 \log_{10} \left[(x_u - x_i)^2 + (y_u - y_i)^2\right] \tag{4}$$

where the user coordinates are the only unknowns. When a sufficiently large number of $C/N_0$ measurements is available ($N \geq 2$), it is possible to determine the user position for example by minimizing the following cost function

$$J(x, y) = \sum_{i=0}^{N-1} \left[\left(\frac{C}{N_0}\right)_i - K_i + \frac{1}{2}\alpha 10 \log_{10} \left[(x - x_i)^2 + (y - y_i)^2\right]\right]^2 \tag{5}$$

where $N$ is the number of $C/N_0$ measurements available. In this way, the user coordinates are obtained as

$$(x_u, y_u) = \arg \min_{x,y} J(x, y) \tag{6}$$

(5) is the Mean Square Error (MSE) between the measured $C/N_0$ values and the model in right-hand side of (4). The minimization problem in (6) can be solved using a gradient descent algorithm where the initial user position can be set equal to the average of the pseudolite coordinates. This approach is commonly used in the literature and additional details can be found in [9] and in the references therein.

The MSE algorithm detailed above was tested using $C/N_0$ measurements collected with the u-Blox receiver. However, it has been verified that as the $C/N_0$ values were approaching zero, significant errors were introduced. This effect simply reflects the fact that low $C/N_0$ measurements are unreliable. In the limit case, measurements with $C/N_0$ values close to zero should be removed. For this reason, cost function (5) was modified to de-weight measurements characterized by low $C/N_0$ values. The new cost function adopted in this paper is

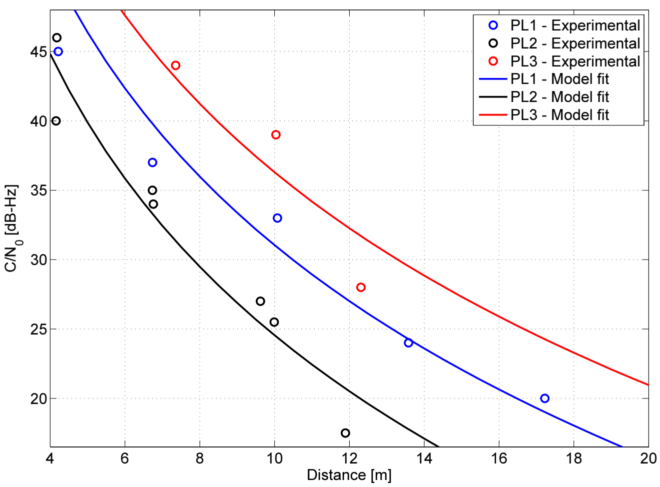


Fig. 4. Calibration results interpolating $C/N_0$ values as a function of distance.

defined as:

$$J_w(x,y) = \sum_{i=0}^{N-1} \left(\frac{C}{N_0}\right)_i \cdot$$
$$\left[\left(\frac{C}{N_0}\right)_i - K_i + \frac{1}{2}\alpha 10 \log_{10}\left[(x-x_i)^2 + (y-y_i)^2\right]\right]^2 \quad (7)$$

where the subscript "w" was added to denote the fact that the cost function is now a form of Weighted MSE (WMSE) where each term in the summation in (7) is weighted by its relative $C/N_0$. The WMSE algorithm significantly outperformed the standard method and for this reason only sample results relative to the WMSE approach are presented.

### A. Algorithm Calibration

The RSS positioning algorithms detailed above assume the knowledge of the parameters

$$\alpha, K_i \quad \text{for } i = 0, ..., N-1.$$

These parameters are however unknown and have to be determined using a calibration stage. This calibration process was performed by exploiting the knowledge of the control point positions and their distances from the pseudolites . The calibration of the RSS parameters was performed by fitting $C/N_0$ measurements obtained in a trial data collection. These measurements were used only for calibration purposes and different tests were conducted to assess the potentialities of the asynchronous pseudolite navigation system. The data collected during the calibration phase allowed the one to plot the average $C/N_0$, observed at a specific control point, as a function of distance. The different measurements were then fitted according to model (2). Experimental points are depicted in Fig. 4 as small empty circles whereas continuous lines represent the interpolated model. Model (2) effectively interpolates experimental measurements and the values obtained for the different parameters are provided in Table III. Note that a single $\alpha$ has been determined for all the measurements whereas $K_i$ is a parameter specific to each pseudolite . In particular, $\alpha$ is determined by the environment where the pseudolite signals are broadcast and thus a common parameter can be used. On the other side, the adoption of pseudolite specific $K_i$ is justified by the fact that the USRPs are not calibrated and each device can transmit a slightly different power. This phenomenon clearly emerges from Fig. 4 which shows that pseudolite 2 has a lower $K_i$ than pseudolite 1 and pseudolite 3: experimental data lay on parallel curves and the adoption of a single $K_i$ it is not possible. Using the values reported in Table III, it was finally possible to perform indoor location using $C/N_0$ measurements.

TABLE III
PARAMETERS FOR RSS POSITIONING OBTAINED THROUGH CALIBRATION.

| Parameter | Value |
|---|---|
| $\alpha$ | 5.1 |
| $K_1$ | 82 dB(Hz·m) |
| $K_2$ | 75.5 dB(Hz·m) |
| $K_3$ | 87.2 dB(Hz·m) |

## V. EXPERIMENTAL RESULTS

In this section, sample results obtained using the Realtek RTL2832U front-end and the u-blox LEA-6T receiver are presented. Two different aspects are considered. At first, sample results obtained using the Realtek RTL2832U front-end are presented. These results demonstrated that pulsed pseudolite signals can be effectively processed using low-cost devices and an SDR approach. $C/N_0$ measurements obtained using the Realtek device show that it is possible to identify when the user is moving (change of control point) or if he is static. These findings confirm the preliminary results obtained in [6] that adopted a high-fidelity Radio Frequency Signal Analyzer (RFSA) for the data collection. Positioning results are discussed in the second part of the section. In this case, measurements from the u-blox receiver are used as input to the WMSE based algorithm described in Section IV.

### A. Signal Processing Results

In order to process the raw I/Q samples provided by the Realtek RTL2832U front-end, the pseudolite Matlab receiver

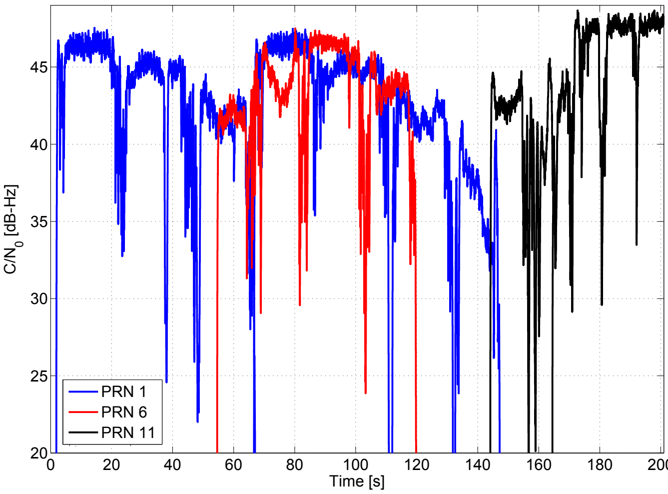


Fig. 5. $C/N_0$ estimated using a Matlab pseudolite receiver for the 3 pseudolite signals broadcast during a dynamic test where the user is progressively moving along the corridor depicted in Fig. 1. The user stopped at each control point for about 20 seconds.

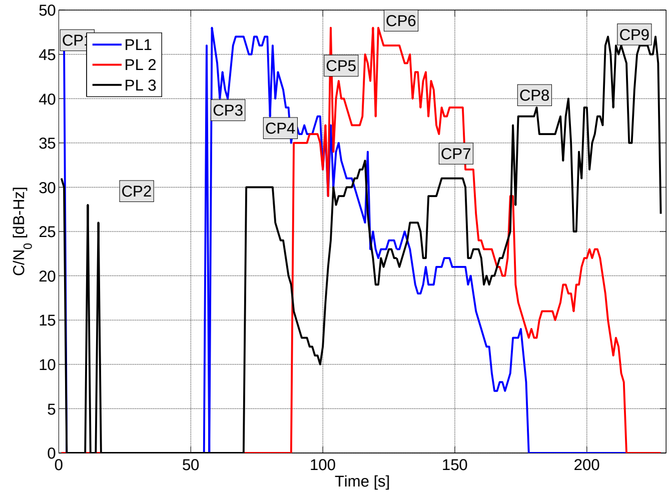


Fig. 6. Estimated $C/N_0$ values as a function of time. These measurements are used for demonstrating RSS positioning.

developed in [6] has been modified. The original pseudolite receiver included acquisition, pulse synchronization and tracking. The Realtek RTL2832U front-end is characterized by a local oscillator of very low quality which causes frequency drifts and introduces large apparent dynamics on the estimated signal Doppler frequencies. For this reason, the frequency uncertainty space searched by the acquisition stage has been significantly extended. Moreover, the reaction of the local oscillator to dynamic changes and shocks caused frequent loss of locks. For this reason, a reacquisition stage was introduced. In this way, it was possible to effectively process the pseudolite signals and extract valid $C/N_0$ measurements. Sample results are provided in Fig. 5 that shows the $C/N_0$ values estimated for the 3 pseudolite signals broadcast during a dynamic test. In this case, the user was progressively moving along the corridor depicted in Fig. 1. The user stopped at each control point for about 20 seconds. From the results obtained in Fig. 5, it is possible to easily identify the different control points and distinguish the dynamic and static periods of the tests. In this respect, the $C/N_0$ values provided in Fig. 5 clearly show the feasibility of proximity based positioning. Potential errors can easily be corrected using careful power control or combining measurements from different pseudolites . Although during the test the user never entered the rooms equipped with the pseudolites , the $C/N_0$ plot in Fig. 5 support the conclusion that room recognition can be achieved easily with the technology developed.

Despite this results, the high sensitivity of the Realtek RTL2832U local oscillator to dynamics and vibrations make it unsuitable for dynamic scenarios. In particular, special processing is required for handling large frequency uncertainties and frequent loss of lock. For this reason, the $C/N_0$ measurements generated by the u-blox receiver have been preferred for the computation of the user position using the algorithm detailed in Section IV.

### B. Positioning Results

In this section, positioning results obtained using u-blox $C/N_0$ measurements are presented. The tests, conducted after the calibration phase, involved a user moving along the trajectory defined by the control points depicted in Fig. 1.

The $C/N_0$ values provided by the u-blox receiver are plotted as function of time in Fig. 6; during the first phase of the test (0-55 second), the user was outside the building and the pseudolite signals were attenuated by walls and thus were too weak to be acquired. For this reason, no information was available to perform RSS positioning. Therefore results are presented only for the portion of the test where valid measurements were available. The $C/N_0$ values seem to represent the user's location correctly; for instance, the blue curve relative to pseudolite 1 shows $C/N_0$ values reaching their maximum (48 dB-Hz) when the user is on the third control point placed in front of the door of the room where the first pseudolite was placed. When the user passes the third control point a progressive decrease in $C/N_0$ is observed.

The $C/N_0$ values of Fig. 6 are provided here to facilitate interpretation of the results obtained in the position domain and discussed below. In particular, anomalous behavior is noted in correspondence of control point 7.

The $C/N_0$ values depicted in Fig. 6 were used to compute the user's position based on the WMSE criterion discussed in Section IV. The position fixes are shown in Fig. 7 along with the pseudolite and control point coordinates which were represented in the local frame East North (EN). The origin of the local frame is pseudolite 1, the y axis is coincident with the North direction whereas the x axis is directed along the East-West direction.

The trajectory along the corridor was characterized by a displacement of about 25 meters in the North-South direction and only 5 meters in the East-West direction. Note that the location of the pseudolites was dictated by the geometry of the building which is mainly oriented along the North-South direction. Consequently, the three devices are able to provide useful information mainly for the estimation of the North coordinate. In fact, they were mainly distributed along the user trajectory. Thus the position fixes depicted in Fig. 7 are mainly scattered along the East-West direction. As already mentioned, the geometry along the East-West direction is quite poor due to the pseudolite displacement, i.e. the difference between pseudolite 1 and pseudolite 2 East coordinates is less than half a meter, and the only device placed on the opposite side of the building was pseudolite 3. For this reason, the error along the East-West direction reaches a maximum value of about 10 meters. This occurs in correspondence of control point 7 which is characterized by anomalous $C/N_0$ measurements as highlighted in Fig. 6. When excluding the position fixes corresponding to control point 7, the East-West error is however lower than 5 meters. This result is considered positive given the geometry of the system and the quality of the measurements. Quality checks of the measurements were not performed and no additional constraints, such as mapping and time domain filtering, were implemented. Improved performance is expected by enhancing the WMSE algorithm developed by introducing constraints and measurements from other sensors.

In order to better understand the results obtained, position results depicted in Fig. 7 are further considered in Fig. 8. From Fig. 8, it emerges that most of the position fixes are confined inside the building. Moreover, most of the errors occur when the user is close to control point 7. This type of behavior was consistent among different data collections and it is probably due to changes of propagation conditions caused by the presence of the stairs door which leads to the ground floor. The position fixes provided by the u-blox receiver

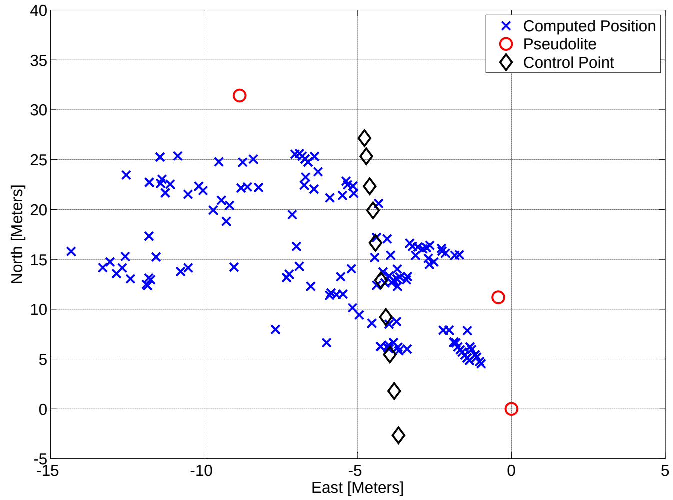


Fig. 7. Horizontal position estimates obtained using the RSS based algorithm.

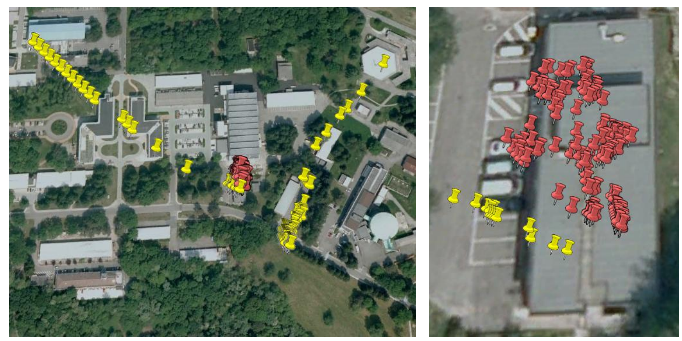

Fig. 8. Position results obtained using the u-blox receiver. Red markers indicate position fixes obtained using pseudolite measurements. Yellow markers corresponds to the position estimates provided by the u-blox receiver and obtained using GPS only measurements.

and obtained using only GPS measurements are also shown in Fig. 8. The u-blox receiver is unable to provide meaningful results in an environment as harsh as the one considered for the pseudolite testing. To demonstrate the impact of the pseudolite geometry on the position solution, performance along the North direction is analyzed separately in Fig. 9, where the blue line represents the estimated North coordinates and the red dotted line represents the North coordinates of the control points expressed in the EN frame. From Fig. 9, it emerges that the maximum error for the North coordinate has a maximum values of about 7 meters in correspondence of control point 7. Again, the error is probably due to the anomalous behavior of the $C/N_0$ values shown in Fig. 6. For the remaining part of test the North component is characterized by metric order accuracy.

These results are extremely encouraging and justify further investigations to fully exploit the benefits of asynchronous

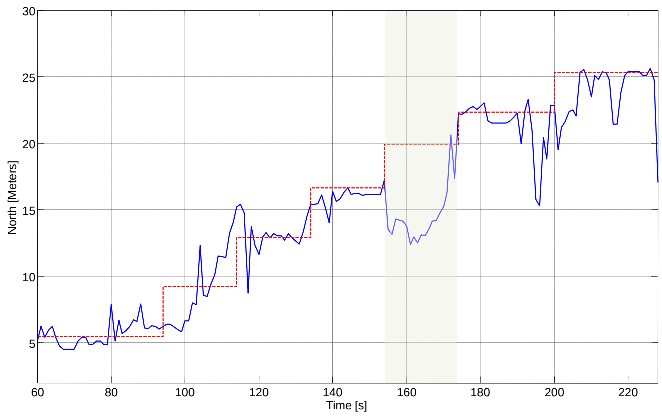


Fig. 9. North coordinate evolution as a function of time. The red dotted line indicates the position of the control points.

pseudolite navigation.

## VI. Conclusions

In this paper, the potentiality of an asynchronous pseudolite system were investigated. Three asynchronous pseudolites were deployed in an office building and $C/N_0$ measurements were used to determine the user position with an RSS-based approach.

The use of asynchronous pseudolites significantly reduces the design and implementation constraints of the system. The different devices can operate independently and the system can be implemented in frequency bands different from the GNSS ones since inter-frequency biases are no longer relevant. The tests conducted for this work were performed in the GPS L1 frequency band only to reduce the development time and exploit GNSS receivers already on the market.

From the analysis, it emerged that 3 pseudolites are sufficient to enable indoor navigation in an office area of about 350 square meters with meter level accuracy. These results are particularly encouraging, since they were obtained without exploiting map constraints and prior knowledge of the user position. The inclusion of such constraints and the propagation of the user position, for example using a Kalman filter, are currently under investigation and will be analyzed in future work.

## Acknowledgments


This work has been partially supported by the European Commission in the framework of the EPCIP 2010 project (C.32253-2011 NFP - AWP CIPS 2010).


## References


[1] B. D. Elrod and A. J. Van Dierendonck, *Pseudolites* in *Global Positioning System, Theory and Applications*. American Institute of Aeronautics and Astronautics (AIAA), Jan. 1996, vol. 2, ch. 2, pp. 51–79.

[2] H. S. Cobb, “GPS pseudolites: Theory, design and applications,” PhD Thesis, Stanford University, http://waas.stanford.edu/ wwu/papers/gps/PDF/Thesis/StuCobbThesis97 .pdf, September 1997.

[3] S. Söderholm and T. Jokitalo, “Synchronized pseudolites – the key to indoor navigation,” in *Proceedings of the International Technical Meeting of the Satellite Division of the Insititute of Navigation (ION GPS 02)*, Portland, Or., 24 – 27 Sep. 2002.

[4] D. Manandhar, K. Okano, M. Ishii, H. Torimoto, S. Kogure, and H. Maeda, “Development of ultimate seamless positioning system based on QZSS IMES,” in *Proc. of the 21st International Technical Meeting of the Satellite Division of The Institute of Navigation (ION GNSS 2008)*, Savannah, GA, September 2008, pp. 1698–1705.

[5] K. Yajima, “IMES (indoor messaging system) the solution for deep indoor navigation,” in *Proceedings of the 23rd International Technical Meeting of The Satellite Division of the Institute of Navigation ION GNSS*, Portland, OR, September 2010, pp. 1779–1799.

[6] D. Borio, E. Cano, and G. Baldini, “Sychronization of pulsed pseudolite signals: Analysis and comparison,” in *Proc. of the 25th International Technical Meeting of The Satellite Division of the Institute of Navigation (ION GNSS)*, Nashville, TN, Sep. 2012, pp. 482–493.

[7] D. Borio and C. O’Driscoll, “Design of a general pseudolite pulsing scheme,” *IEEE Trans. Aerosp. Electron. Syst.*, pp. 1–16, 2013, accepted for pub.

[8] I. Kraemer, P. Dykta, R. Bauernfeind, and B. Eissfeller, “Android GPS jammer localizer application based on $C/N_0$ measurements and pedestrian dead reckoning,” in *Proc. of the 25th International Technical Meeting of The Satellite Division of the Institute of Navigation ION/GNSS*, Nashville, OR, Sep. 2012, pp. 3154–3162.

[9] P. Tarrio, A. M. Bernardos, , and J. Casar, “Weighted least squares techniques for improved received signal strength based localization,” *Sensors*, vol. 11, pp. 8569–8592, Sep. 2011.

[10] P. Tarrio, A. M. Bernardos, J. Besada, and J. Casar, “A new positioning technique for RSS-based localization based on a weighted least squares estimator,” in *IEEE International Symposium on Wireless Communication Systems (ISWCS).*, 2008, pp. 633–637.

[11] T. A. Stansell, “RTCM SC-104 recommended pseudolite signal specification,” *NAVIGATION: Journal of The Institute of Navigation*, vol. 33, no. 1, pp. 42–59, Spring 1986.

[12] N. Patwari, J. Ash, S. Kyperountas, A. Hero III, R. L. Moses, and N.S.Correal, “Locating the nodes: cooperative localization in wireless sensor networks,” *IEEE Signal Process. Mag.*, vol. 22, no. 4, pp. 54–69, Jul. 2005.

[13] M. Hatay, “Empirical formula for propagation loss in land mobile radio services,” *IEEE Trans. Veh. Technol.*, vol. 29, no. 3, pp. 317–325, Aug. 1980.

[14] L. Scott, “J911: The case for fast jammer detection and location using crowdsourcing approaches,” in *Proc. of the 24th International Technical Meeting of The Satellite Division of the Institute of Navigation ION/GNSS*, Portland, OR, Sep. 2011, pp. 1931–1940.

[15] O. Isoz, A. T. Balaei, and D. Akos, “Interference detection and localization in the GPS l1 band,” in *Proc. of the International Technical Meeting of The Institute of Navigation (ITM/ION)*, San Diego, CA, Jan. 2010, pp. 925–929.